Spin excitations of a model itinerant ferromagnetic film: Spin waves, Stoner excitations, and spin-polarized electron-energy-loss spectroscopy

M. P. Gokhale and D. L. Mills
Department of Physics, University of California, Irvine, California 92717
(Received 2 June 1993)

We discuss the spin excitations of a simple model of an ultrathin ferromagnetic film, in which the magnetic moment bearing electrons are itinerant in character. The one-band Hubbard model, treated in mean-field theory, forms the basis of the discussion. The spin excitations are treated by means of the random-phase approximation. We find spin-wave modes of standing wave character, and a spectrum of Stoner excitations influenced strongly by size effects. While the dispersion relations of the standing spin-wave modes appear as expected from a localized-spin model, there are substantive differences between the itinerant- and localized-spin cases. An example is the number of spin-wave modes evident in the appropriate spectral density functions, for each wave vector. We use a previously developed formalism of spin-polarized electron-energy-loss scattering (SPEELS) to compute SPEELS spectra for our model film. In addition to a broad feature with origin in Stoner excitations, we find clear and relatively intense spin-wave loss peaks.

I. INTRODUCTION

Ultrathin (few atomic layer) films can be synthesized from constituents that exhibit magnetic order in bulk form. In most cases, the films exhibit long range magnetic order also. Currently there is great interest in the study of the magnetism and the electronic structure of these ultrathin films, with emphasis on the often considerable differences with bulk magnetic matter.

Films of a material such as Fe can display long range ferromagnetic order when they are as thin as a monolayer,[1] and the Curie temperature can be appreciable. For a quasi-two-dimensional magnetic material, even a modest amount of anisotropy can drive the transition temperature up to rather substantial values,[2] though the Mermin-Wagner theorem requires the transition temperature to vanish in two dimensions, if the spin-spin interactions are perfectly isotropic. In real materials, by virtue of either magnetic dipole interactions or spin-orbit effects, anisotropy is always present. At temperatures well below the anisotropy induced transition temperature, the low-lying elementary excitations of the material are spin waves. It is assumed often that these may be described within a localized spin picture,[3] although in many cases (such as Fe and the other $3d$ transition metals) the magnetic moment bearing electrons are surely itinerant in nature. In the latter case, one may argue on general grounds[4] that spin waves remain the low-lying excitations. But nonetheless a proper description of these excitations should be based on a fully itinerant model, if one has applications to transition metals in mind.

This paper presents a theoretical study of the spin excitations in a model of an itinerant electron film with a ferromagnetic ground state. We use our results to generate theoretical descriptions of the contributions to electron-energy-loss spectra from spin-flip scatterings of beam electrons off the film. These model spectra outline the conditions we believe are required to observe spin-wave features in the electron-energy-loss spectrum of ultrathin ferromagnetic films, and by inference from ferromagnetic surfaces. Experiments to date have yet to observe such loss features.

For many years, it has been known that a band picture of the magnetic electrons in itinerant ferromagnets indeed yields spin waves as the low-lying "magnetically active" excitations.[4] However, in addition to spin waves, one also obtains a spectrum of spin-flip single particle excitations referred to often as Stoner excitations.[5] A proper theory must provide an account of both the spin waves, and the Stoner excitations of the ultrathin film, within a single framework. While the Stoner excitations have been studied by the method of spin-polarized electron-energy-loss scattering (SPEELS) on magnetic surfaces and in ultrathin films,[6] their companions in the spectral density, the spin waves have yet to be seen, as noted above.

There are experimental methods that have been used extensively to study such spin waves in ultrathin ferromagnetic films. These are inelastic light scattering (Brillouin scatering)[7] and ferromagnetic resonance.[8] The modes excited in such studies have wavelengths parallel to the surface that are very long compared to the lattice constant. A consequence is that the exchange contribution $Dk_{\parallel}^2$ to the excitation energy is very small, where D is the exchange stiffness and $k_{\parallel}$ is the wave vector parallel to the surface. The modes studied by both techniques have excitation energies dominated by the combination of Zeeman energy, magnetic anisotropies, and magnetic dipole-dipole interactions. The experiments provide detailed data on the nature of anisotropies in such films, but at present we have no direct information on the exchange stiffness. Electron-loss spectroscopy can excite modes with a wave vector sufficiently large for exchange to dominate the excitation energy. Such studies, if successful, can thus provide quantitative data on a key physical property of these materials. In recent years, electron-loss spectroscopy (and He scattering as well) have provided

detailed microscopic information on surface phonons, and analogous experiments on spin waves would be of great interest.

In our results, we find distinct differences between the description of standing spin waves which emerge from the itinerant model, and that provided by the Heisenberg picture of localized spins. Such differences would be evident in electron-loss studies of the ultrathin films. We elaborate on this point below.

There have been past theoretical discussions of spin waves in itinerant ferromagnetic films, and on surfaces. Some years ago, Griffin and Gumbs[9] calculated spin waves in an itinerant electron ferromagnet to find a high-frequency surface spin-wave branch, with a frequency that remained finite and very large as $k_{\parallel}\rightarrow 0$, a behavior which contrasts dramatically from that found in a localized spin picture. Some time later, Mathon noted that this result is incompatible with considerations of spin rotation invariance.[10] He demonstrated, with a single band model rather like that used here, that a description of spin excitations out of a proper self-consistently generated ground state necessarily yields results compatible with spin rotation invariance. We note that, some years earlier, the same issue arose in a closely related area,[11] where a detailed description was given of how results compatible with spin rotation invariance are achieved in the long wave limit, within the random-phase approximation. While aspects of our present results do differ from those obtained in a localized spin picture, they are fully compatible with the requirements of spin rotation invariance.

This paper is organized as follows. Section II discusses the properties of the Hubbard model description of an itinerant bulk ferromagnet. While the general features to be described here have been known for many years,[5] we provide explicit numerical results that will prove useful in our examination of ultrathin films. Section III discusses the properties of the ground-state electron configuration for ultrathin films, and gives our results for the spin excitations from the ground state. Section IV examines the theory of inelastic scattering of electrons from spin excitations. Here we examine the conditions we believe must be realized to observe spin-wave loss features in inelastic electron scattering.

II. THE HUBBARD MODEL DESCRIPTION OF SPIN EXCITATIONS IN THE INFINITE CRYSTAL

As remarked in the Introduction, our analysis is based on the use of the one-band Hubbard model, as a means of simulating the ground-state properties and the spin excitations in the ultrathin film. In this section, we present studies of these properties in the infinitely extended crystal.

The full Hamiltonian is

$$H=-t\sum_{l,\delta}\sum_{\sigma}c_{l\sigma}^{+}c_{l+\delta\sigma}+U\sum_{l}n_{l\uparrow}n_{l\downarrow}\ , \tag{1}$$

where t is the hopping matrix element between nearest neighbors, U is the on-site Coulomb repulsion, and $n_{l\sigma}$ is the number operator for site l, for electrons with spin σ.

We shall use a mean-field description of the ground state. For these purposes, an effective single-particle Hamiltonian is generated by the replacement

$$n_{l\sigma}\rightarrow\langle n_{l\sigma}\rangle+\delta n_{l\sigma}\ , \tag{2}$$

where $\langle n_{l\sigma}\rangle$ is the ground-state expectation value of the operator $n_{l\sigma}$, and $\delta n_{l\sigma}=(n_{l\sigma}-\langle n_{l\sigma}\rangle)$ formally describes fluctuations about the mean value. For the calculations presented in this section, for the infinite crystal, $\langle n_{l\sigma}\rangle=\langle n_{\sigma}\rangle$, independent of l. When we turn to the film in the next section, this will depend on l_z, the layer index. The effective Hamiltonian is generated by keeping only terms linear in $\delta n_{l\sigma}$.

Thus,

$$H_{\text{eff}}=-U\sum_{l}\langle n_{l\uparrow}\rangle\langle n_{l\downarrow}\rangle+T+U\sum_{l\sigma}\langle n_{l,\sigma}\rangle n_{l\sigma}\ , \tag{3}$$

where T, the kinetic energy, is the hopping term in Eq. (1). The second and third terms of Eq. (3) describe a one-electron Hamiltonian, and the first term corrects for the fact that when the single-particle energies are summed up, the interaction energy is double counted.

One proceeds, then, by solving for $\langle n_{\uparrow}\rangle$ and $\langle n_{\downarrow}\rangle$ in a self-consistent manner. It is well known that in mean-field theory,[5] one finds paramagnetic solutions with $\langle n_{\uparrow}\rangle=\langle n_{\downarrow}\rangle=\langle n\rangle$ for $U<U_c$, and ferromagnetic solutions are admitted for $U>U_c$, where $U_c=1/N(E_F)$, with $N(E_F)$ the density of states at the Fermi level, per spin direction. This is referred to often as the Stoner criterion. In Fig. 1(a), as a function of U, and for the bcc lattice, we show the magnetic moment in the ground state, for a particular choice of total electron occupancy $n=\langle n_{\uparrow}\rangle+\langle n_{\downarrow}\rangle$. In the figure $W=16t$ is the one-electron bandwidth. We see the onset of ferromagnetism near $U/W=1$. There should be a sharp onset, with $\langle n_{\uparrow}\rangle-\langle n_{\downarrow}\rangle\sim(U-U_c)^{1/2}$ in mean-field theory. The small bit of rounding has its origin in the use of a finite mesh in the Brillouin zone integrations.

Of interest is the dynamic susceptibility $\chi(\mathbf{Q},\Omega)$, which described the spin excitations out of the ground state. Here and in Sec. III, we employ the random-phase approximation (RPA) to describe this quantity. In the bulk of the material, and in the RPA, $\chi(\mathbf{Q},\Omega)$ is given by the well-known expression[5]

$$\chi(\mathbf{Q},\Omega)=\frac{\chi_0(\mathbf{Q},\Omega)}{1-U\chi_0(\mathbf{Q},\Omega)}\ , \tag{4a}$$

where

$$\chi_0(\mathbf{Q},\Omega)=\frac{1}{N}\sum_{\mathbf{k}}\frac{f(\mathbf{k}\uparrow)-f(\mathbf{k}+\mathbf{Q},\downarrow)}{E(\mathbf{k}+\mathbf{Q},\downarrow)-E(\mathbf{k}\uparrow)-\Omega-i\eta}\ . \tag{4b}$$

Here $f(\mathbf{k}\sigma)$ is the Fermi-Dirac function, and

$$E(\mathbf{k}\sigma)=E_0(\mathbf{k})+U\langle n_{-\sigma}\rangle \tag{5}$$

is the one-electron energy for electrons with spin σ, where

$$E_0(\mathbf{k})=-t\sum_{\delta}e^{i\mathbf{k}\cdot\delta}\ . \tag{6}$$

The elementary excitations of the system are found

from poles in $\chi(\mathbf{Q},\Omega)$. We have a continuum of single-particle excitations of electron-hole character, wherein the electron flips its spin in the course of the excitation process. These are referred to commonly as Stoner excitations. For a given choice of $\mathbf{Q}$, the band of Stoner excitations extends from Ω_m to Ω_M, where

$$\Omega_m = \min[E(\mathbf{k}+Q\downarrow) - E(k\uparrow)]$$

and

$$\Omega_M = \max[E(\mathbf{k}+\mathbf{Q}\downarrow) - E(\mathbf{k}\uparrow)] .$$

Here $\mathbf{k}$ is scanned over the Brillouin zone. As $\mathbf{Q}\rightarrow 0$, we have $\Omega_M \rightarrow \Omega_m = U(\langle n_\uparrow \rangle - \langle n_\downarrow \rangle)$.

There are, in addition, collective excitations, which are the spin waves. These are isolated poles of $\chi(\mathbf{Q},\Omega)$, outside the band of Stoner excitations.[5] In Fig. 1(b), for $\langle n_\uparrow \rangle + \langle n_\downarrow \rangle = 1.75$ and for a particular choice of U, we show the spin-wave disperison relation, and the frequency domain of the Stoner excitations. It should be remarked that here and elsewhere in the paper, ζ is a reduced wave vector along the direction from Γ to X. At the zone boundary, $\zeta = 1$. The spin-wave branch lies quite low in frequency, compared to the exchange splitting $U(\langle n_\uparrow \rangle - \langle n_\downarrow \rangle)$ between the bands, which equals roughly 7.5 units in this example. (We measure energy in units of the hopping integral t.) The inset shows the spin-wave dispersion at small wave vectors. The quadratic variation with wave vector shows clearly here.

In the transition metal ferromagnets, the spin waves lie rather low in frequency, as in this example. To illustrate by bulk Fe, the exchange splitting is approximately 2 eV.[6] The exchange stiffness D is roughly 3.0×10^{-17} eV cm^2. The excitation energy of a spin wave with wave vector in the range of 10^8 cm^{-1} is then 0.25 eV, very small compared to the exchange splitting as in Fig. 1.

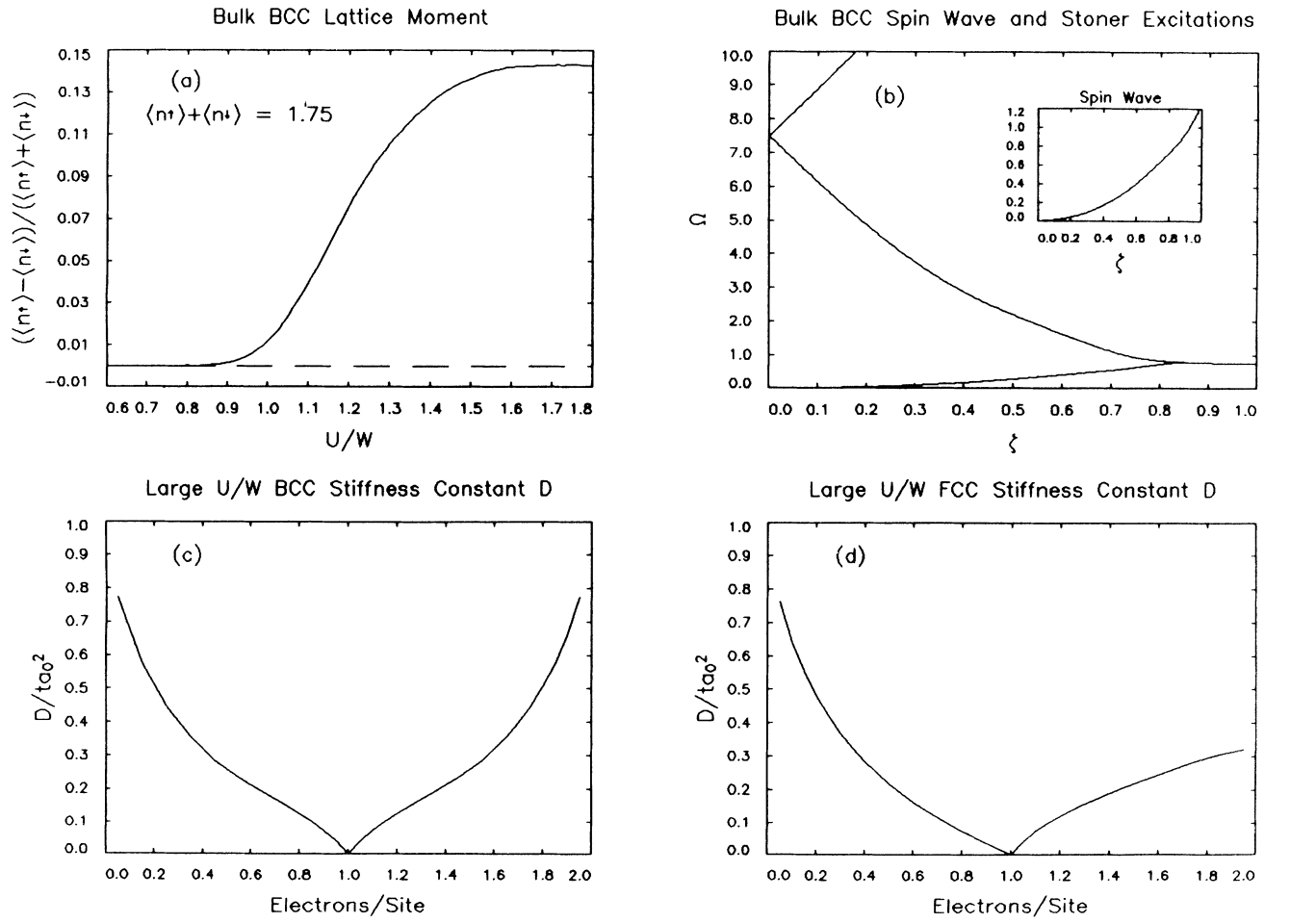

FIG. 1. This figure summarizes the results of our calculations for the Hubbard model, applied to the infinite crystal. We have (a) the bulk magnetic moment in the ground state of the bcc lattice, as a function of U/W, with W the bandwidth; (b) for $U=30$, the bcc lattice, and $\langle n_\uparrow \rangle + \langle n_\downarrow \rangle = 1.75$, we show as a function of wave vector the bands of Stoner excitations (cross hatched region), and the spin-wave dispersion relation. The frequency Ω, and U are measured in units of the hopping integral t. The wave vector $\mathbf{Q}$ is directed along (100), and ζ is a reduced wave vector whose value equals unity at the Brillouin zone boundary. The inset demonstrates the quadratic dependence of the spin wave frequency with wave vector, for small wave vectors. In (c) and (d), we show the variation of the spin wave exchange stiffness with the number of electrons per site.

The above discussion is based on the notion that the ground state of the one-band Hubbard model is, in fact, ferromagnetic in nature, for the bcc three-dimensional lattice, and the occupancy considered. It is surely the case that within our mean-field description of the system, the ground state is indeed ferromagnetic. Furthermore, we see from Fig. 1(b) that all spin excitations out of the ground state have positive definite excitation energies. Our ground state is thus stable with respect to small amplitude deviations of any wave vector from perfect ferromagnetic alignment.

However, as far as we know, it is not established rigorously that the exact ground state of the 3D Hubbard model is, in fact, ferromagnetic. For exact half-filling and the bcc lattice, in the limit of large U, it is well known that we have antiferromagnetism. There appears to be no clear statement one can make (particularly in three dimensions) off half-filling, and for general U, about the ground state. Nagaoka[12] has shown that as $U\rightarrow\infty$, and with one hole present in an otherwise half-filled band, a strong ferromagnetic state is the ground state, for the bcc and other 3D lattices. A review of the literature on discussions of the true ground state of the Hubbard model is given in Sec. I of a recent paper by von der Linden and Edwards.[13] We note that in a more recent paper,[14] Henderson, Oitmaa, and Ashley argue that, at finite temperatures, ferromagnetism indeed occurs for the one-band Hubbard model, over a substantial portion of the phase diagram.

Quite clearly, within the framework of our mean-field description, we cannot address the question of the nature of the exact ground state. It will suffice for our purposes, however, if the ferromagnetic (mean-field) state is locally stable, i.e., stable against small amplitude deviations from ferromagnetism. We can then discuss its spin excitations, as just illustrated in a particular case, and use the model as the basis for a simple description of an itinerant ferromagnet.

We have explored the stability of the menn-field ground state as a function of electron occupancy n, for both the fcc and the bcc lattice, to find stable ferromagnetism save at half-filling. We illustrate this in Figs. 1(c) and 1(d), where we give the variation of spin-wave exchange stiffness with electron occupancy n, in the limit $U\rightarrow\infty$. The exchange stiffness is positive definite everywhere, except at $n=1$ (half-filling) where it vanishes. Similar results are found for finite U. At a fixed value of n, we find that D is a monotonically increasing function of U, to vanish as $(U-U_c)^2$, as the Stoner value U_c is approached form above.

We now turn to our results for the film of a finite number of layers.

III. GROUND-STATE PROPERTIES AND SPIN-EXCITATIONS IN THE HUBBARD FILM

The discussion of this section will be divided into two parts. We examine first the nature of the ground states we find for the Hubbard film, and then we turn to our RPA results for the spin dynamics of a selected case.

A. The ground-state properties

The basic scheme for the mean-field analysis of the ground state was described in Sec. II. We have a film with N layers, and the occupancies of the various sites $\langle n_{l\uparrow}\rangle$ and $\langle n_{l\downarrow}\rangle$ then depend on the layer index l_z. The up spin electrons thus see a layer-dependent self-consistently determined potential $U\langle n_{lz\downarrow}\rangle$ from the down spin electrons, while the down spin electrons see $U\langle n_{lz\uparrow}\rangle$ from the up spins. We thus have $2N$ quantities to be found in a self-consistent manner.

The single-particle eigenfunctions are Bloch states with respect to the two spatial variables parallel to the surface. These then have the form

$$\psi_{\mathbf{k}_\parallel\alpha,\sigma}(\boldsymbol{l}_\parallel,l_z)=\exp(i\mathbf{k}_\parallel\cdot\boldsymbol{l}_\parallel)\phi_{\mathbf{k}_\parallel\alpha,\sigma}(l_z)\ . \tag{7}$$

Here $\mathbf{k}_\parallel$ lies within the approporatie two-dimensional Brillouin zone and α is an index which ranges from 1 to N, which labels the Bloch states associates with the particular wave vector $\mathbf{k}_\parallel$. The eigenfunctions $\phi_{\mathbf{k}_\parallel\alpha,\sigma}(l_z)$ are normalized so that

$$\sum_{lz}|\phi_{\mathbf{k}_\parallel\alpha,\sigma}(l_z)|^2=1\ . \tag{8}$$

One begins with a guess for an initial set of $\langle n_{lz\sigma}\rangle$, then through an appropriate iteration scheme determines these from the requirement

$$\langle n_{lz\sigma}\rangle=\frac{1}{N_s}\sum_{\mathbf{k}_\parallel,\alpha}|\phi_{\mathbf{k}_\parallel\alpha;\sigma}(l_z)|^2 f(\mathbf{k}_\parallel\alpha;\sigma)\ , \tag{9}$$

where

$$f(\mathbf{k}_\parallel\alpha;\sigma)=(\exp\{\beta[E(\mathbf{k}_\parallel\alpha;\sigma)-\mu]\}+1)^{-1}$$

is the Fermi-Dirac function, and $E(\mathbf{k}_\parallel\alpha;\sigma)$ the energy eigenvalue associated with the state in Eq. (7). The Fermi energy μ is determined by the requirement that the total number of electrons be fixed. In our numerical work, β is chosen as $0.1t$, with t the hopping integral. Then $f(\mathbf{k}_\parallel\alpha;\sigma)$ is a continuous function of its argument. We find this small amount of smoothing useful in the numerical work.

Many self-consistent calculations have been performed for finite jellium slabs, where the electron density varies continuously with distance from the surface. For example, one of the present authors has been involved in earlier studies of electron density profiles in GaAs films, on the basis of such a picture.[15] From the point of view of numerical analysis, there are substantive differences between the Hubbard film studies (or any electronic structure study based on a lattice) and the jellium analyses. In the latter case, the eigenvalues $E(\mathbf{k}_\parallel\alpha,\sigma)$ have a trivial dependence on $\mathbf{k}_\parallel$. One has

$$E(\mathbf{k}_\parallel\alpha,\sigma)=(\hbar^2k_\parallel^2/2m)+\epsilon_{\alpha,\sigma}\ ,$$

where $\epsilon_{\alpha,\sigma}$ is found from a simple one-dimensional Schrödinger equation. Also, the l_z dependent function $\phi_{\mathbf{k}_\parallel\alpha;\sigma}(l_z)$ is independent of $\mathbf{k}_\parallel$. In this case, it is quite easy to perform the integration on $\mathbf{k}_\parallel$ in Eq. (9) analytically, thus leaving only the sum on α. Here (as in full elec-

tronic structure calculations for real materials) we have to perform the numerical integration on $\mathbf{k}_{\parallel}$. For slabs in the thickness range 6–12 layers, we find 200 points in the irreducible one-eighth of the surface Brillouin zone leads to accurate results. We have explored ground-state properties of films as thick as forty layers, to find highly accurate results. For such thick films, we required the order of 1000 points in the irreducible piece of the surface zone.

The Hubbard film admits an array of ground states with rich and varied properties. We illustrate this in Fig. 2, where we give various examples of the ground-state spin arrangements in films. In Fig. 2(a), we have a ferromagnetic film with enhanced surface moments in the outer layer. These results, at least in a qualitative sense, are similar to those which emerge from full electronic structure calculations of Fe surfaces.[16] Notice the moments in the second layer are reduced a bit from their bulk value, on our example. In Fig. 2(b), we show the moment distribution for the band occupancy and value of U used to generate Figs. 1(a) and 1(b). Here we have a reduction of the moment in the surface, and an enhancement in the second layer.

There are also solutions in which the magnetic moment resides in mostly the outer layer or two, while in the bulk one has small moments. We show an example in Fig. 2(c), for an fcc film with (100) surface. Here one has primarily surface magnetism. It has been suggested also that in a certain thickness range (5–10 atomic layers), Fe films on Cu(100) exhibit magnetism only in the outer surface.[17] A state such as that in Fig. 2(c) may in fact also be compatible with the data.

There is also great curernt interest in Fe/Cr superlattices; of course, the Fe films are ferromagnetic, and in the bulk Cr is antiferromagnetic. The (100) planes in antiferromagnetic Cr are ferromagnetic sheets, with moments that alternate in sign as one moves parallel to the [001] direction. While the electronic structure of the Cr films is yet to be established, recent experimental studies of Cr overlayers on Fe(100) show they exhibit antiferromagnetism.[18,19] We show in Fig. 2(d) a self-consistent calculation of the ground-state spin densities for one unit cell in a "Hubbard superlattice," where one constituent is ferro-

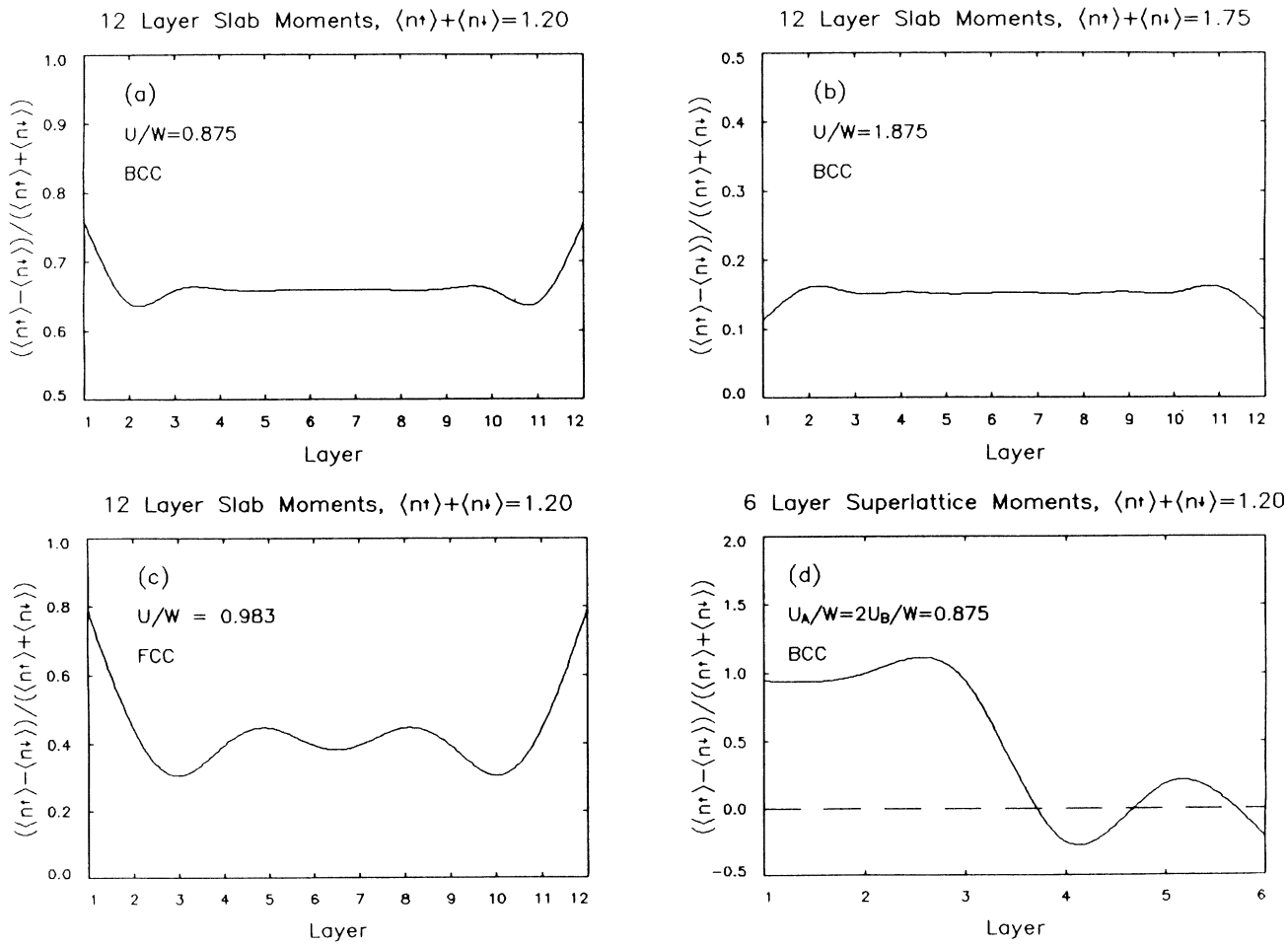

FIG. 2. We show, for various band fillings and choices of U, ground-state spin densities in the Hubbard film with 12 layers. In (a) we have enhanced surface moments, while in (b) the moments in the outer layer are smaller than those in the bulk, whereas those in the second layer are enhanced. In (c), we have an example of a case where there is magnetism mostly in the surface, and in (d), where periodic boundary conditions are used, we have a ferromagnetic film adjacent to an antiferromagnetic film. This is the unit cell of a model superlattice.

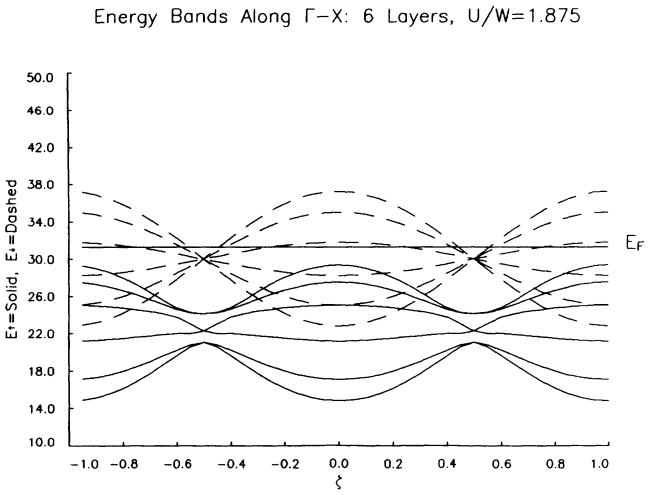

FIG. 3. For the case where the total electron occupancy is 1.75, we show the electron "minibands" along the direction Γ-X in the surface Brillouin zone. Energy is measured in units of the hopping integral t. The position of the Fermi level is indicated. The quantity ζ is the reduced wave vector used earlier, and $\zeta=\pm 1$ is the zone boundary. The up spin minibands are full lines, and down spin minibands are dashed lines.

magnetic, and one is antiferromagnetic. We remark that, for this case, we have studied structures as thick as 40 layers, to be certain we indeed have one ferromagnetic and one antiferromagnetic constituent. This case may serve as a model for Fe/Cr superlattices, or Fe/Cr sandwiches.

These examples show that the magnetic properties of the Hubbard film are very rich. We can use this model as the basis for initial studies of the spin excitations for magnetic films of diverse character.

In the next section, we present our study of the spin dynamics of ferromagnetic Hubbard films. For the initial studies presented here, we have chosen the example in Fig. 2(b). As one sees from Fig. 1(c), for this value of the band filling, the spin-wave exchange stiffness D is rather large. From the point of view of the numerical work described in the next subsection, this is an advantage.

We conclude this section with Fig. 3, which shows the spin-up and spin-down "minibands" [the eigenvalues $E(\mathbf{k}_\parallel\alpha,\sigma)$, for $\mathbf{k}_\parallel$] along the $\bar{\Gamma}$-$\bar{X}$ direction in the surface Brillouin zone for for a six-layer Hubbard slab.

There is one intriguing feature in Fig. 3. Notice that when $\zeta=\pm 0.5$, there is a sixfold degeneracy in the down spin eigenvalues. For this choice of ζ, the various planes of the film decouple, and the eigenfunctions $\phi_{\mathbf{k}_\parallel\alpha,\sigma}(l_z)$ are localized in one particular plane. Each of the states has energy $U\langle n_{l\uparrow}\rangle$, and $\langle n_{l\uparrow}\rangle\equiv 1$ for each of the six layers, since the up spin band is full, as one can see from the position of the Fermi level in Fig. 3. There are splittings in the up spin energies at $\zeta=\pm 0.5$, since now $\langle n_{l\downarrow}\rangle$ varies wth layer number, while $\phi_{\mathbf{k}_\parallel\alpha,\uparrow}(l_z)$ remains localized in l_z. A study of the energy splittings at $\zeta=\pm 0.5$ by valence-band photoemission would thus provide direct information on the spatial inhomogeneity of the magnetic moments in the film. While the spatial variation of the magnetic moments in real materials is unlikely to have such a direct and simple influence on the structure of the electron minibands, it would be of great interest to explore this issue for a more realistic picture of the electronic structure.

B. Spin excitations in the Hubbard film: Spin waves and the Stoner excitations

As remarked earlier, we shall base our discussion on the use of the RPA, with mean-field ground states such as those described in the previous section as the basis. We begin with general remarks.

In the infintiely extended crystal, the dynamic susceptibility displayed in Eq. (4a), provides (in the RPA) a description of the reesponse of the spin system to an external magnetic field of wave vector $\mathbf{Q}$ and frequency Ω, applied perpendicular to the magnetization in the ferromagnetic ground state. The applied field is assumed circularly polarized, and $\chi(\mathbf{Q},\Omega)h$ is the amplitude of the transverse magnetization excited by the external field, where h is the strength of the external field.

We confine our attention in this section to ferromagnetic films, with N layers, as discussed in the previous subsection. Once again, a magnetic field of frequency Ω, circularly polarized, is applied perpendicular to the magnetization. It has the wave vector $\mathbf{Q}_\parallel$ parallel to the surface, and we wish to allow its spatial variation normal to the surface to be quite general. The amplitude of the magnetic field thus has the form

$$h(\boldsymbol{l}_\parallel l_z;t)=h(l_z)\exp[i\mathbf{Q}_\parallel\cdot\boldsymbol{l}_\parallel-i(\Omega+i\eta)t]\ . \tag{10}$$

If $\langle s_+(l_z)\rangle$ is the amplitude of the transverse response excited in layer l_z by the above field, then linear response theory provides a relation between $\langle s_+(l_z)\rangle$ and $h(l_z)$. One has

$$\langle s_+(l_z)\rangle=\sum_{l_z'}\chi(\mathbf{Q}_\parallel\Omega;l_z l_z')h(l_z')\ . \tag{11}$$

It is by now a standard matter to express $\chi(\mathbf{Q}_\parallel\Omega;l_z l_z')$ in terms of the relevant spin operators of the system. The various spin excitations associated with the wave vector $\mathbf{Q}_\parallel$ appear as poles of $\chi(\mathbf{Q}_\parallel\Omega;l_z l_z')$ in the frequency plane. The spin-wave modes of the film will appear as poles in the frequency domain below the Stoner excitation region, as we shall see.

Once the dynamic susceptibility $\chi(\mathbf{Q}_\parallel\Omega;l_z l_z')$ is known, through use of a formalism we have developed earlier,[20] it is possible to calculate the contribution to the electron energy loss cross section, from processes in which the beam electron flips its spin. In Eq. (22) of Ref. 20, the probability the electron loses energy $\hbar\Omega$ through a spin-flip process is seen to be proportional to a sum over the Fourier transform of a certain correlation function

$$\langle s_+(\mathbf{Q}_\parallel l_z';t)s_-(\mathbf{Q}_\parallel l_z;0)\rangle\ ,$$

with $s_\pm(\mathbf{Q}_\parallel l_z;t)$ operators associated with transverse spin fluctuations in layer l_z, of wave vector $\mathbf{Q}_\parallel$. We have the identity

$$\int_{-\infty}^{+\infty}\frac{dt}{2\pi}e^{i\Omega t}\langle s_+(\mathbf{Q}_\parallel l_z';t)s_-(\mathbf{Q}_\parallel l_z;0)\rangle = [1+n(\Omega)]\,\mathrm{Im}[\chi(\mathbf{Q}_\parallel\Omega;l_z'l_z)]\ . \quad (12)$$

Here

$$n(\Omega)=[\exp(\hbar\Omega/k_BT)-1]^{-1}$$

is the Bose-Einstein function.

Thus, once we obtain the response functions defined in Eq. (11), through use of Eq. (12) and the multiple scattering theory of SPEELS developed earlier, we may generate a theoretical SPEELS spectrum for spin-flip scattering of an external beam of low-energy electrons from the film. The results of such a study is the topic of Sec. IV of the present paper. Here, our attnetion is directed toward the analysis of $\chi(\mathbf{Q}_\parallel\Omega;l_zl_z')$ and the information one can extract from this function.

Within the RPA, the full response function $\chi(\mathbf{Q}_\parallel\Omega;l_zl_z')$ is readily generated once $\chi_0(\mathbf{Q}_\parallel\Omega;l_zl_z')$ of the electrons moving on the self-consistent ground-state potential is synthesized. One has

$$\chi_0(\mathbf{Q}_\parallel\Omega;l_zl_z')=\frac{1}{N}\sum_{\mathbf{k}_\parallel,\alpha\alpha'}\phi^*_{\mathbf{k}_\parallel\alpha,\uparrow}(l_z)\phi_{\mathbf{k}_\parallel\alpha,\uparrow}(l_z')\phi_{\mathbf{k}_\parallel+\mathbf{Q}_\parallel\alpha'\downarrow}(l_z)\phi^*_{\mathbf{k}_\parallel+\mathbf{Q}_\parallel\alpha',\downarrow}(l_z')\left[\frac{f(\mathbf{k}_\parallel\alpha,\uparrow)-f(\mathbf{k}_\parallel+\mathbf{Q}_\parallel\alpha',\downarrow)}{E(\mathbf{k}_\parallel+\mathbf{Q}_\parallel,\alpha';\downarrow)-E(\mathbf{k}_\parallel\alpha,\uparrow)-\Omega-i\eta}\right]\ . \quad (13)$$

The major computational task is to generate an accurate description of χ_0, which serves as the kernel in the equation from which the full susceptibility is generated. If we let $U(l_z)$ be the strength of the Coulomb repulsion experience by electrons in layer l_z [Fig. 2(d) provides an example of a model in which the electron-electron interaction is not identical in all layers], then the full susceptibility is found from

$$\chi(\mathbf{Q}_\parallel\Omega;l_zl_z')=\chi_0(\mathbf{Q}_\parallel\Omega;l_zl_z')+\sum_{l_z''}\chi_0(\mathbf{Q}_\parallel\Omega;l_zl_z'')U(l_z'')\chi(\mathbf{Q}_\parallel\Omega;l_z''l_z')\ . \quad (14)$$

Once χ_0 is known accurately, it is a simple task to invert the $N\times N$ set of equations just given, and find the full susceptibility.

Before we present the results of our study, we comment on aspects of the computation of χ_0. First of all, the calculations reported below employ a small but finite value of the infinitesimal η which appears in Eq. (14). For resolving the spin-wave structures shown below, values of η as small as 0.05, in units of the hopping integral t, were employed. For a given $\mathbf{Q}_\parallel$, we then calculated χ_0 and χ in frequency intervals of $0.005t$. The $\mathbf{k}_\parallel$ space grid described in regard to the ground-state calculations proved adequate. We proceeded by integrating over the full surface Brillouin zone. While the calculation could be reduced to an integration over one-eighth of the surface zone, for each choice of $\mathbf{Q}_\parallel$, this requires a symmetry analysis that differs for each choice of $\mathbf{Q}_\parallel$. In the end, an integration over the entire surface Brillouin zone seemed more straightforward, though in future work we shall address this question. In many of the calculations, we employed SUN workstations. One to two days of computation time were required for a six-layer slab, for each value of $\mathbf{Q}_\parallel$. Several SUN workstations were used in parallel to generate results for a 12 layer slab.

Considerations of spin rotation invariance require that for $\mathbf{Q}_\parallel=0$ we have a spin-wave mode with zero frequency.[10,11] As we shall see shortly, we find such a mode in our work, and at $\mathbf{Q}_\parallel=0$, its frequency is zero with high accuracy. To achieve this result, we believe it important to use the same $\mathbf{k}_\parallel$ grid in both the mean-field description of the ground state, and the calculation of χ_0. The point is the following. The use of a "conserving approximation" in a many-body description of the spin dynamics ensures that constraints imposed by considerations such as spin rotation invariance are properly incorporated into the scheme. The RPA constitutes such a "conserving approximation," for a system whose ground state is approximated by our mean-field method. If, in the calculation of the various $\langle n_{l\sigma}\rangle$ for the slab, we use a regular $\mathbf{k}_\parallel$ grid, in effect we are quantizing $\mathbf{k}_\parallel$ in the same fashion as we would for a slab of N layers, but with finite extent in the xy plane. Periodic boundary conditions have then been applied in the xy plane. If a different grid were used for the calculation of χ_0 (possibly a finer grid to improve accuracy), in effect one would be describing the spin dynamics of an object whose spatial extension in the xy plane differs from that for which the $\langle n_{l\sigma}\rangle$ have been generated. In such a situation, there is an incompatibility between the description of the spin dynamics, and the description of the ground state. This leads to violations of constraints imposed by spin rotation invariance. Thus, if one wishes to improve the accuracy of one aspect of the calculation by using a finer grid, one must incorporate the new grid in the other plase at the same time.

In Fig. 4(a), we show the results of calculations for the six-layer bcc film with occupancy 1.75 electrons/site. We are plotting

$$\rho(\mathbf{Q}_\parallel\Omega;l_zl')=\mathrm{Im}[\chi(\mathbf{Q}_\parallel\Omega;l_zl_z')]$$

for the choice $l_z=l_z'=1$. The wave vector is along the $\bar{\Gamma}$-$\bar{X}$ direction. The four peaks above $\Omega=2$ are Stoner excitations. These may be viewed as particle-hole excitations, within the "miniband" structure displayed in Fig. 3. There are low-frequeny features which lie well below $\Omega=1.0$. These are the standing spin-wave modes of the slab. As one increases the wave vector, the spin waves increase their frequency, and move toward the Stoner features.

While much of our subsequent discussion will be centered on the spin-wave structures, the Stoner excitation

region is of very considerable interest as well. As one sees from Fig. 1(b), in the bulk for example, the exchange splitting between the up and down spin bands is $U(\langle n_\uparrow \rangle - \langle n_\downarrow \rangle) = 7.5$; in the bulk, as the wave vector $\mathbf{Q} \to 0$, one finds that $\mathrm{Im}[\chi_0 \mathbf{Q}, \Omega)]$ degenerates into a delta function in frequency, at the exchange splitting $U(\langle n_\uparrow \rangle - \langle n_\downarrow \rangle)$.

Now if, in our film we are to regard the Stoner excitations as a reflection of the transition energies between the electron "minibands" of Fig. 3, then our calculated Stoner spectrum should bear a close similarity to $\mathrm{Im}[\chi_0(\mathbf{Q}_\parallel \Omega; 11)]$; this describes the spectrum of spin-flip particle-hole excitations for the film, in the one-electron limit. For the film, it plays the role of $\mathrm{Im}[\chi_0(\mathbf{Q}, \Omega)]$ in the bulk. In Fig. 4(b), we show $\mathrm{Im}[\chi_0(\mathbf{Q}_\parallel \Omega; 11)]$ at $\zeta = 0$ for the six-layer film. Its structure is complex, but clearly the "center of gravity" of the features shown is quite close to the bulk exchange splitting of 7.5. Comparison between the Stoner region of Fig. 4(a) with Fig. 4(b) shows that the particle-hole final-state interactions included in the RPA shift the Stoner structure dramatically, to lower energy. There is thus a question about using such features in SPEELS spectra as a measure of the average exchange splitting in the one electron energy bands. We note that in Ni, the peak of the Stoner spectrum is near 300 meV,[21] while density functional calculations yield 600 meV,[22] larger by roughly a factor of 2.

In Fig. 4(a), the low-frequency spin-wave structures are not resolved fully. In Fig. 4(c), we show this region in detail. The lowest spin-wave mode has a frequency of exactly zero, as required by spin rotation invariance. We then see two higher-lying modes. If we regard these modes as standing spin waves with frequency $D(\pi n/N)^2$, with D the bulk spin-wave stiffness [Fig. 1(b)], we obtain quite a reasonable account of the frequencies shown in Fig. 4(c), with the choice $n = 0$, 1, and 2. Figure 4(d) shows the spin-wave excitation spectrum for $\zeta = 0.4$. Quite clearly, the modes have dispersion, and increase in frequency with $\mathbf{Q}_\parallel$. In Fig. 5, we show the variation in frequency of these modes with $Q_\parallel$ along the $\bar{\Gamma}$-$\bar{X}$ direction. These curves are fitted nicely by $D[Q_\parallel^2 + (\pi n/N)^2]$.

One striking feature evident in Fig. 4 is that for the

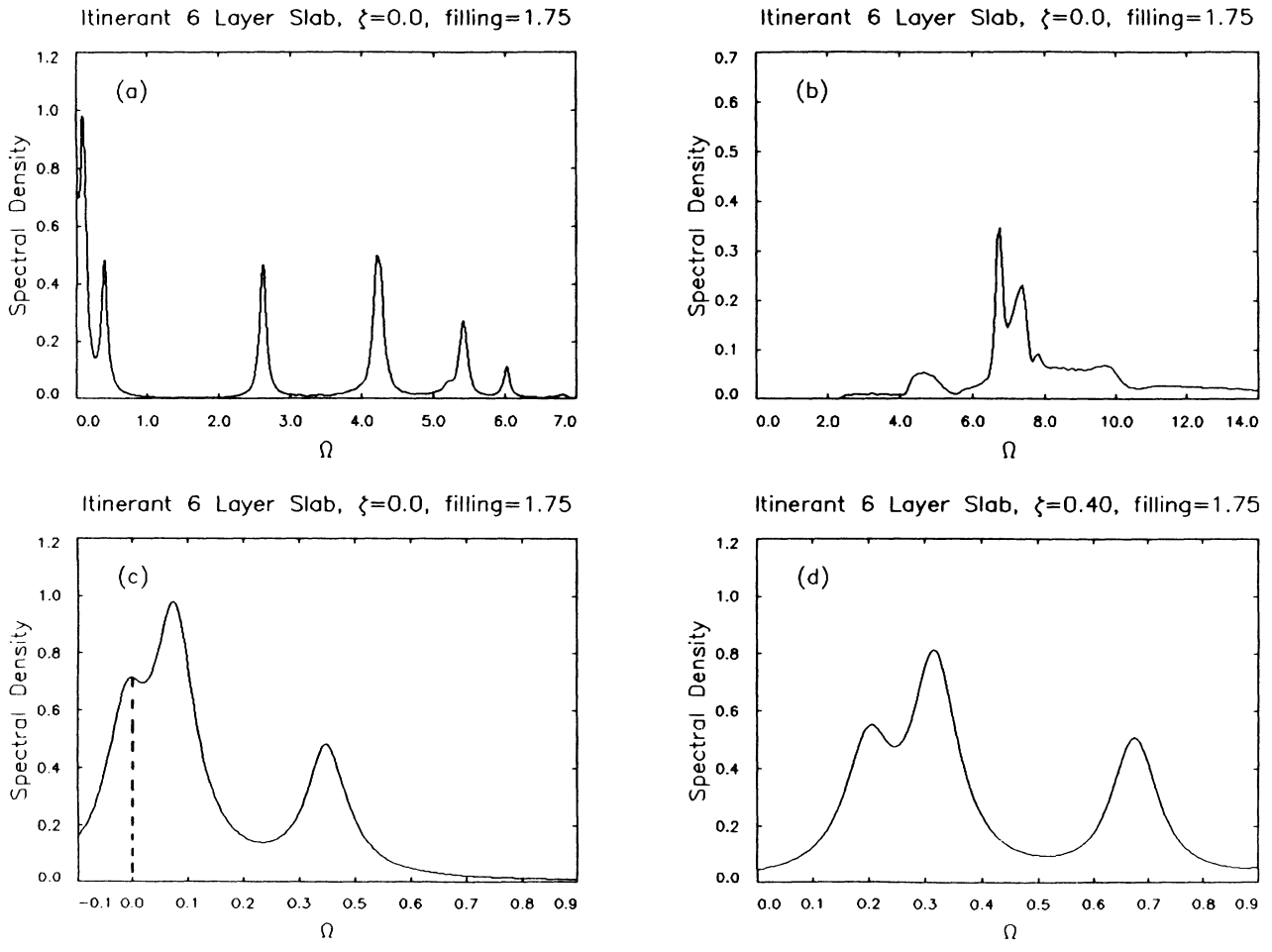

FIG. 4. We show the frequency variation of spin fluctuations in the outermost layer of a six-layer bcc film with (100) surface. We plot, for values of the reduced wave vector ζ along $\bar{\Gamma}$-$\bar{X}$, $\rho(\mathbf{Q}_\parallel \Omega; 11) = \mathrm{Im}[\chi(\mathbf{Q}_\parallel, \Omega + i\eta, 11)]$. We show (a) the spectral density $\rho(\mathbf{Q}_\parallel \Omega; 11)$ for the interacting electrons for $\zeta = 0$, and (b) the free electron spectral density $\rho_0(\mathbf{Q}_\parallel \Omega; 11)$ again for $\zeta = 0$. In (c), we have an enlargement of the low-frequency spin-wave structure shown in (a), and in (d) an enlargement of the similar feature for $\zeta = 0.4$. Frequency is measured in units of the hopping integral. Recall that $\zeta = 1$ at the zone boundary.

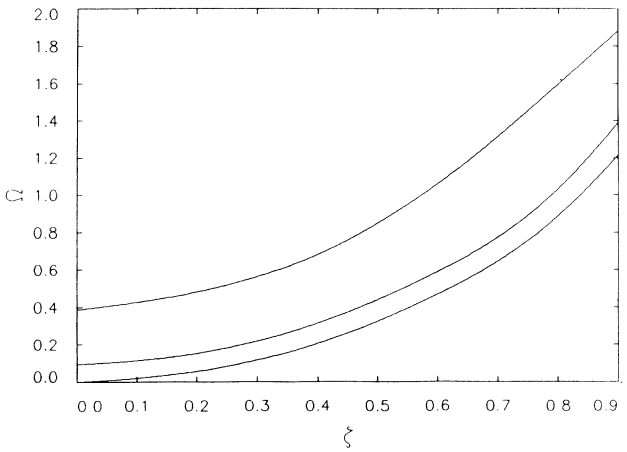

FIG. 5. The dispersion relation of the standing spin-wave modes illustrated in Figs. 4(c) and 4(d). The frequency is measured in units of the hopping integral t. The reduced wave vector ζ assumes the value 1 at $\bar{X}$, in the surface zone.

six-layer itinerant ferromagnet, we find only three standing wave modes for each value of $\mathbf{Q}_\parallel$. For a Heisenberg film of six layers, quite obviously one has six modes. It is not the case here that the three missing modes just have very small amplitude in the outer surface layer. One may see this by scanning $\rho(\mathbf{Q}_\parallel\Omega;l_z l_z)$ for all values of l_z. We have examined the parity of the spin-wave modes shown in Fig. 4, to find the lowest mode has even parity, the second mode odd parity, and the third mode even parity. The standing spin waves of a Heisenberg film necessarily alternate in parity, as one moves through the sequence. We have examined model films of various thicknesses, to always find the number of spin-wave modes is less than the number of layers. An eight layer film has four modes, a twelve-layer film has six modes, and a seven-layer film has three modes.

There is, as far as we know, no requirement that in an itinerant ferromagnetic film with N layers, there must be precisely n standing wave spin-wave modes. The excitation spectrum of the itinerant system is clearly more complex than that of a localized spin ferromagnet, modeled as a Heisenberg system. In the latter case, the *only* excitations are spin waves. One sees quite trivalially that in a Heisenberg film of N layers, there are precisely N modes associated with each wave vector $\mathbf{Q}_\parallel$. The itinerant electron film has, in addition, the Stoner excitations, which, at least for small $\mathbf{Q}_\parallel$, lies above the spin-wave region. In some sense, the Stoner excitations account for a reasonable fraction of the oscillator strength in the total spectrum of spin excitations for any particular $\mathbf{Q}_\parallel$, and our results show that a consequence is a fewer number of standing spin-wave modes.

One may see this as follows. Suppose we examine the wave-vector–dependent susceptibility of a bulk ferromagnet, at $T=0$. This is the function $\chi(\mathbf{Q},\Omega)$ described, for the itinerant system, by our Eq. 4(a). Now if we have a lattice of Heisenberg spins of length S, it is an elementary exercise to show that, if $\omega_s(\mathbf{Q})$ is the frequency of a spin wave of wave vector $\mathbf{Q}$,

$$\chi(\mathbf{Q},\Omega)=\frac{S}{\omega_s(\mathbf{Q})-\Omega} \ . \tag{15}$$

The *only* feature in $\chi(\mathbf{Q},\Omega)$ is the spin-wave pole, and this accounts for all the integrated strength in the spectral density.

Now for the itinerant system, as we have seen, there are indeed spin waves that appear as poles of $\chi(\mathbf{Q},\Omega)$, but in addition there are bands of Stoner excitations [Fig. 1(b)]. Consider the behavior of $\chi(\mathbf{Q},\Omega)$ lfor the itinerant system, near the spin-wave pole at $\Omega=\omega_s(\mathbf{Q})$. We have, near the pole,

$$\chi(\mathbf{Q},\Omega)\cong\frac{(\langle n_\uparrow\rangle-\langle n_\downarrow\rangle)r(\mathbf{Q})}{\omega_s(\mathbf{Q})-\Omega} \ , \tag{16}$$

where

$$r(\mathbf{Q})=-\frac{\chi_0(\mathbf{Q},\omega_s(\mathbf{Q}))}{U(\partial\chi_0/\partial\Omega)|_{\omega_{s(\mathbf{Q})}}(\langle n_\uparrow\rangle-\langle n_\downarrow\rangle)} \ . \tag{17}$$

One may show easily that as $\mathbf{Q}\to 0$, $r(\mathbf{Q})\to 1$, and Eq. (16) becomes identical in content to Eq. (15). But as $\mathbf{Q}$ increases, $r(\mathbf{Q})$ decreases with $\mathbf{Q}$; oscillator strength is "extracted" from the spin wave, and transferred into the spectrum of Stoner excitations.

We believe that the short-wavelength standing spin-wave modes fail to appear in our spectral densities because their oscillator strength is very small, by virture of an analogue for the film of the phenomenon just described. There is then a substantial difference between the spin-wave excitations of the Heisenberg film and the itinerant electron ferromagnetic film.

We illustrate this point explicitly in Fig. 6, where we compare spectral density functions for the six-layer itinerant film, and a six-layer Heisenberg film set up to mimic the itinerant picture. In the Heisenberg film, the size of the spin S in each layer was adjusted to reproduce the magnetic moment profile in the ground state of the itinerant model [Fig. 2(b)]. The nearest-neighbor exchange interactions J were the same between all neighbors, with strength chosen so the exchange stiffness D which controls the quadratic term in the bulk dispersion relation is the same as that in the itinerant model. In Figs. 6(a) and 6(b), we compare the spectral densities in the first layer,

$$\rho(\mathbf{Q}_\parallel\Omega;11)=\mathrm{Im}[\chi(\mathbf{Q}_\parallel\Omega;11)] \ .$$

Six modes are clearly evident in the Heisenberg case (though the two highest-frequency modes have small amplitudes in the surface). A similar comparison in the second layer is given in Figs. 6(c) and 6(d). The three low-lying modes of the Heisenberg film are quite close in frequency to those of the itinerant film, but the three high-frequency modes are missing in the itinerant case. There is a hint of a fourth mode in Fig. 6(c), but its oscillator strength is small, consistent with the expectation from Eq. (16). The sixth mode in Fig. 6(d) has a large amplitude in layer 3, it should be remarked.

It may be that the high-frequency modes are simply Landau damped, by virtue of their overlap with the spectrum of Stoner excitations [Fig. 1(b)]. It is indeed the

case, based on extrapolation from the dispersion relation of Fig. 5, that these modes would lie within the Stoner continuum. However, in the relevant frequency regions, we find $\mathrm{Im}[\chi_0(\mathbf{Q}_\parallel\Omega;l_z,l_z')]$ to be quite small. As a consequence, we believe Landau damping plays a minor role, for the example given.

We conclude with a comparison of the behavior of $\rho(\mathbf{Q}_\parallel\Omega;11)$ for a 6- and a 12-layer slab. We show spectral densities for $\zeta=0.6$ for these two cases in Fig. 7. A high resolution scan of the spin-wave regime shows there to be six standing spin waves, as noted earlier. The Stoner region is broader, and begins to approach the broad feature observed in earlier experiments.[6] Surely in few layer films, the quantum well nature of the single-particle states should introduce structure into the Stoner region, though no structure with a possible origin in quantum well states has been reported in the literature. This is an exaggeration in our one-band Hubbard model, however. In a real material such as Fe, there are five orbitals per spin direction for each site, rather than the single orbital here. There will thus be $5N$ "minibands" per spin direction, in the same bandwidth, where we have just N. We plan studies of more realistic pictures in the future, with emphasis on the size dependence of structure in the Stoner region, among other issues. In their study of very thin Co films, Idzerda *et al.*[6] see clear structure in the measured spin asymmetry, which they argue has its origin in Stoner excitations. These authors argue its origin lies in bulk band structure features rather than the influence of quantum wells effects. We note that the data were taken on the specular, where dipole coupling enhances the coupling to particle-hole excitations unaccompanied by a spin reversal. This may cloud contributions from spin-flip processes, where dipolar enhancements are missing. A theory developed by one of us[22] shows, however, there are dipole enhanced spin asymmetries in the loss spectrum associated with non-spin-flip losses. These issues are addressed in the discussion presented by Idzerda *et al.*[6]

IV. THEORY OF SPIN-POLARIZED ELECTRON-ENERGY-LOSS SPECTRA OF THE MODEL FILM

The previous section was devoted to a study of the spin fluctuation spectrum of our model film. Here we use a formalism developed earlier by ourselves and Ormeci,[20]

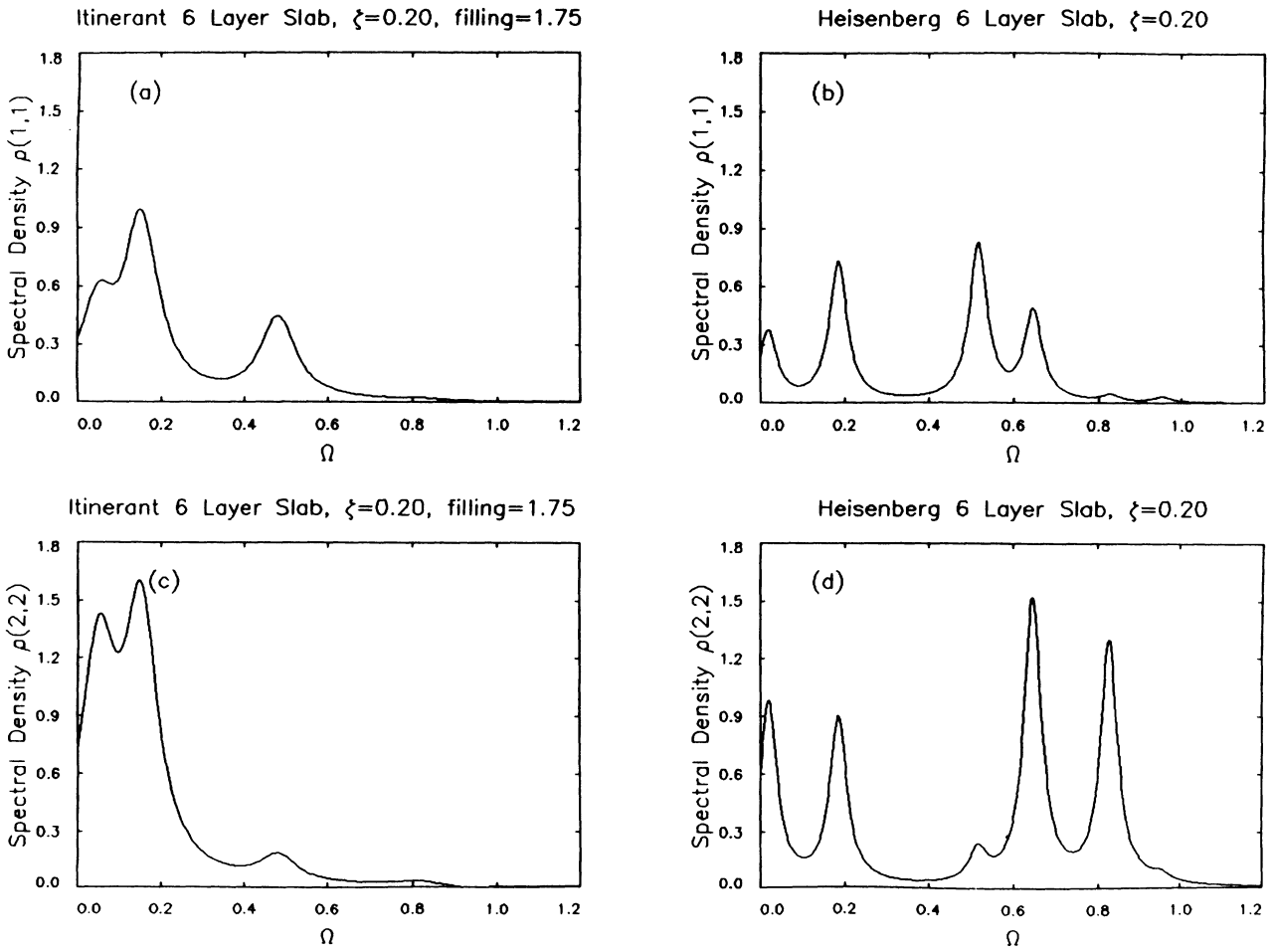

FIG. 6. We compare spectral densities for the localized spin (Heisenberg) model, and the itinerant model, in the spin-wave regime. We have, with $\rho(\mathbf{Q}_\parallel\Omega;l_zl_z)=\mathrm{Im}[\chi(\mathbf{Q}_\parallel\Omega;l_zl_z)]$, (a) $\rho(\mathbf{Q}_\parallel\Omega;11)$ for the six-layer itinerant electron ferromagnet, (b) $\rho(\mathbf{Q}_\parallel\Omega;11)$ for the Heisenberg case, (c) $\rho(\mathbf{Q}_\parallel\Omega;22)$ for the six-layer itinerant electron ferromagnet, and (d) $\rho(vQp\Omega;22)$ for the Heisenberg case. The parameters for the Heisenberg case are chosen as described in the text.

combined with the dynamical susceptibilities described in the previous section to calculate the contribution from spin-flip processes to the electron-energy-loss spectrum from the model films. We comment first on the experiments that motivate these studies.

Spin-polarized electron beams can be used to probe the magnetism at surfaces of magnetically ordered materials, and ultrathin films on substrates. Both the spin dependence of elastic scattering from such materials, and the electron-energy-los spectrum, provide information on magnetic structure and in the latter case, magnetic excitations. We cite examples of electron-loss studies in Refs. 6 and 21. In recent experiments, the spin of the scattered electron is detected. It is then possible to isolate from the data the contribution from losses in which the beam electron spin is flipped in the course of the scattering event. The studies of Abraham and Hopster[6,21] explore such spectra in a remarkably complete manner, for scattering from Ni(110), while Venus and Kirschner explore Fe.[6]

Special interest has been directed toward the component of the loss spectrum in which a beam electron polarized parallel to the minority spin direction experiences a spin flip. If one considers this contribution for a material such as Ni, where (as in the model film explored in the previous section) the majority spin bands are filled in the bulk, by means of an exchange scattering one may create a Stoner excitation wherein a majority spin substrate electron is promoted to empty states in the minority spin band. This provides one access to information on the exchange splittings in the material, though we are unaware of any microscopic calculations that can be compared directly with the data. In the experiments, the Stoner excitations produce a very broad feature in the loss spectrum, with a peak near 300 meV at low temperature. This peak is at an energy smaller than calculated bulk exchange splittings by a factor of 2.[23]

In the same channel, one sees easily that one should expect spin-wave losses in addition to the Stoner excitations. As far as we know, no experimental study has reported spin-wave features in electron-energy-loss studies of magnetically ordered materials. The calculations to be reported below show these features appear in the spectrum with substantial intensity. Thus, we see no clear reason why a suitable experiment cannot observe these excitations.

The quantity we study, as discussed earlier, is $d^2P/d\Omega(\hat{k}_s)d\Omega$, the differential probability the electron will scatter into solid angle $d\Omega(\mathbf{k}_s)$ with energy loss in the range $d\Omega$. This is synthesized from the dynamic susceptibilities $\chi(\mathbf{Q}_\parallel\Omega;l_z l_z')$, and from a multiple scattering description of the propagation of the electron through the crystal. Upon noting the identity in Eq. (12), and the fact that $n(\Omega)\cong 0$, we have from Eq. (22) of Ref. 20,

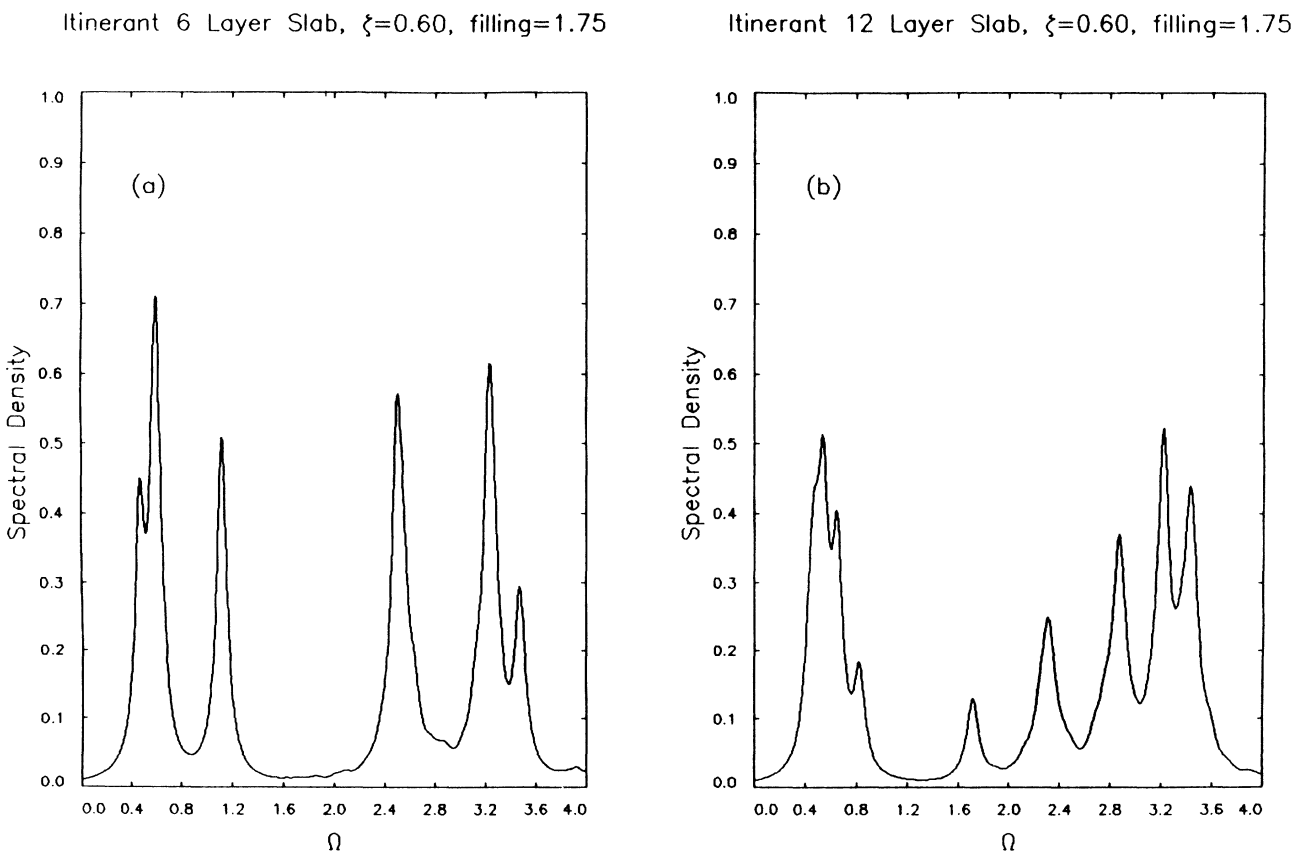

FIG. 7. For the itinerant ferromagnetic film, with occupancy of 1.75 electrons/site and $\zeta=0.60$, we show the spectral density $\rho(\mathbf{Q}_\parallel\Omega;11)$ for (a) the six-layer and (b) the twelve-layer film.

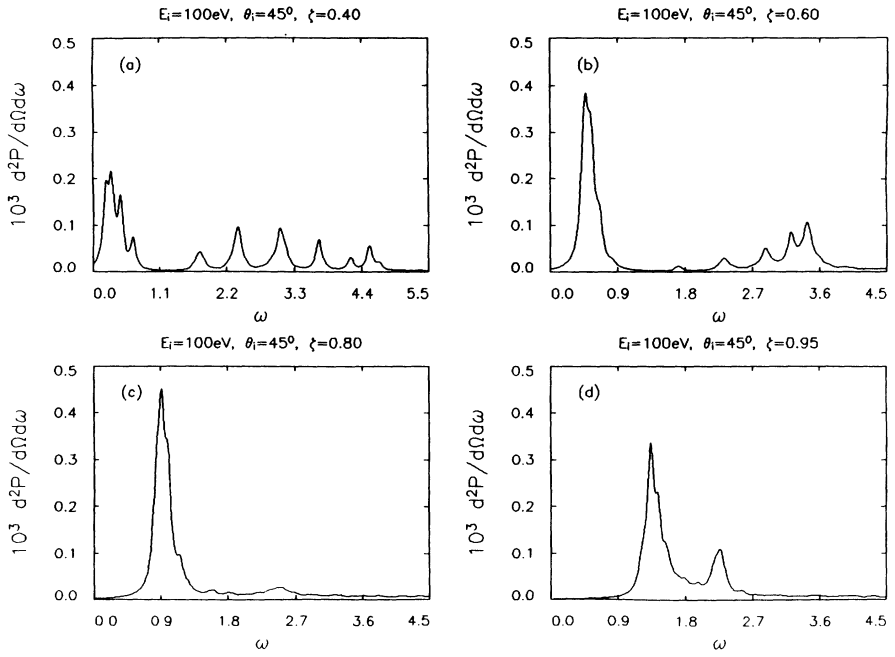

FIG. 8. We show, for the twelve-layer bcc Hubbard film, theoretical values of the spin-flip contribution to the SPEELS spectrum for (a) $\zeta=0.40$, (b) $\zeta=0.60$, (c) $\zeta=0.80$, and (d) $\zeta=0.95$. The electron beam energy is 100 eV.

$$\frac{d^2P}{d\Omega(\hat{k}_2)d\Omega}=\left[\frac{mE_i\cos^2\theta_f}{2\pi^2h^2\cos\theta_i}\right]A_c\sum_{l_z l_z'}\sum_{g}\sum_{g'}A_{l_z}^{(g)}(\mathbf{k}_f\sigma_f,\mathbf{k}_i\sigma_i)A_{l_z}^{(g')}(\mathbf{k}_f\sigma_f,\mathbf{k}_i\sigma_i)\,\mathrm{Im}[\chi(\mathbf{Q}_\parallel\Omega;l_zl_z')]\ . \tag{18}$$

In Eq. (18), $\mathbf{k}_i\sigma_i$ and $\mathbf{k}_f\sigma_f$ are the initial- and final-state wave vector and spin of the beam electron, while E_i, θ_i, and θ_f are the incidient energy and the initial and final angle between the beam electron momenta and the surface normal. A prescription, using multiple scattering theory, for calculating the amplitudes $A_{l_z}^{g}(\mathbf{k}_f\sigma_f;\mathbf{k}_i\sigma_I)$ is given in Ref. 20. The calculations reported below use single site potentials for Fe, as in our earlier study of scattering from Heisenberg spin waves.[20] The details of the potentials have rather little influence on the relative intensity and shape of the features in the loss spectra; as we found earlier,[20] broadly speaking our theoretical SPEELS intensities for Fe are perhaps an order of magnitude larger than for Ni.

In Fig. 8, for four values of the dimensionless wave vector and an electron beam energy of 100 eV, we show our theoretical spin-flip portion of the SPEEL spectrum. For $\zeta=0.4$ and 0.6, the Stoner excitation region, which lies above $\omega=1.5$, is very broad very much as found in the experimental studies. The structure in the Stoner region of the spectrum our calcualtions has its origin in the quantum well nature of the one electron states. As remarked in the previous section, it is not clear at this time whether this structure would survive in a more complete thoery, where the full oribital degeneracy of the magnetic electrons is incorporated. For $\zeta=0.8$ and 1.0 the Stoner portion of the spectrum is weak compared to the spin-wave portion. We will see shortly that this is a special feature associated with this choice of beam energy.

The strong structure in the dimensionless frequency range $\omega\sim0.5$–0.9 has its origin in the standing spin-wave modes. These stand out very prominently, and since the Stoner region has been studied experimentally, these results suggest spin waves can surely be observed.

In Fig. 9, we show theoretically calculated SPEELS spectra, calcualted for the beam energy 30 eV. At the larger values of the momentum transfer ($\zeta=0.8,0.95$), the spin-wave features carry a much reduced fraction of the total scattering strength. Comparison between the results of Figs. 8 and 9 thus illustrate that, by choosing selected beam energies, the spin-wave structures can have their scattering cross section enhanced, relative to the Stoner region. In the earlier studies of surface phonons, the relative contribution of particular phonons to the loss spectrum can be enhanced by the approprite choice of beam energy.[24,25] In the phonon case, the theory is now sufficiently reliable that at least on simple metal surfaces; such energy "windows" may be predicted. While the calculations presented here in Figs. 8 and 9 are based on realistic Fe potentials, our representation of the spin dynamics is at present too oversimplified for the theory to be reliable in this regard.

One may inquire whether the experiments reported earlier could have detected the spin-wave structures. We believe not. Evidently the energy resolution used by Kirschner and Venus and Kirshner[6] was in the range of a few tenths of an eV, as was that of Idzerda and his colleagues. This leads to no difficulty for their studies of the very broad Stoner spectrum of Fe, but the spin waves will lie under the quasielastic peak, and be difficult to resolve. As we noted in Sec. II, if the spin-wave dispersion relation of Fe is extrapolated out to the Brillouin zone boundary, assuming a quadratic dispersion law and the

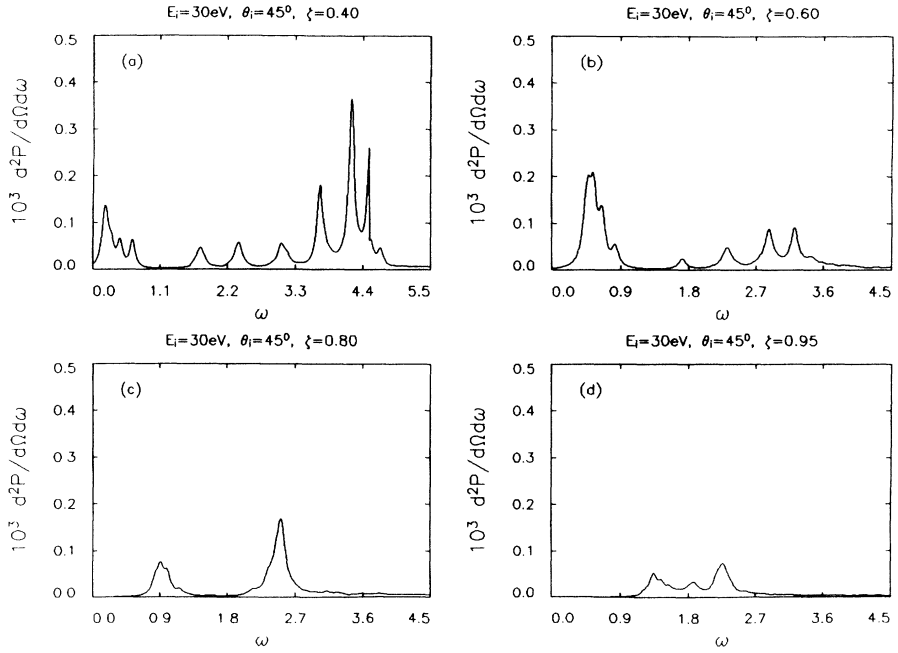

FIG. 9. The same as Fig. 8, except now the beam energy is 30 eV.

bulk exchange constant of Fe, we have an energy of 0.25 eV. Thus, surely the spin waves lie too low in frequency to be resolved in these experiments.

The studies of Abraham and Hopster[6,20] employed much higher resolution, in the range of 80 meV. However, the value of $\mathbf{Q}_{\parallel}$ they explored lies only 10% of the way from the zone center to the zone boundary. Their loss data do not extend below 100 meV. The interesting energy regime lies a bit lower in frequency.

It will be necessary to design an experimental study directed toward the observation of the spin-wave losses. This paper, combined with our earlier work, outlines some key issues such an experiment must address. We conclude by summarizing these conditions.

Surely Fe and/or Ni are the prime candidates, since even films of a few atomic layers have Curie temperatures well above room temperature. The spin-wave exchange stiffness of these 3*d* metals is quite large. This moves the spin-wave structures to high frequency; this should allow one to probe these modes without the extreme high resolution ($\sim$3 meV) used currently in studies of surface phonons.[24,25] Of the two materials, Fe would surely be the optimum choice, since our previous studies of the absolute cross section gave values for scattering from Fe an order of magnitude larger than Ni. We believe an ultrathin film is also the best choice of sample. The standing spin waves produce clean structure in the loss spectrum. In a thick ferromagnet, as illustrated by our earlier work,[20] the breakdown of momentum conservation normal to the surface will lead to a rather broad structure in the loss spectrum produced by spin waves. We argue in the next paragraph that unpolarized electron beams offer substantial advantages over polarized beams; the presence of standing spin-wave structures will improve one's ability to discriminate between spin-wave losses, and the substantial background (from particle hole excitations) that will be present.

The use of polarized beams in the study of Stoner excitations seems quite essential. In the interesting loss region, for the 3*d* transition metal magnets, there are relatively intense, broad features introduced by inelastic scatterings in which the beam electron does not flip.[6] The Stoner excitations, which induce a spin flip, produce a braod structure as well, and the use of polarized beams in combination with a spin detector is required to isolate the spin-flip portion of the loss spectrum. The standing spin-wave loss features from an ultrathin ferromagnetic film will produce rather well-defined structures in the loss spectrum, as we have seen. These should be clearly resolvable from the background, with unpolarized beams. Spin detectors are very inefficient; their efficiency lies in the range 10^{-3}–10^{-4}. Thus, a vast improvement in the detected signal can be achieved if one uses unpolarized beams, and forgoes resolution of the scattered electron spin.

In our earlier study, we compared the spin-wave excitation efficiency for exciting spin waves on Fe, with that for exciting surface phonons.[20] The latter are seen readily in current experiments, on a variety of metals. We found the spin-wave excitation efficiency down by roughly three orders of magnitude, relative to that for exciting surface phonons. Current surface phonon studies employ resolution in the 3 meV range, and beam currents in the range of 100 pA. To study spin waves, one will require higher beam currents to see the signal, but one can tolerate substantially reduced resolution in the study of these relatively high-frequency modes. We note the studies of Stoner excitations employ beam currents in the range of a μA or greater. The use of unpolarized beams with detection efficiency improved greatly by simply counting scattered electrons without resolving their spin, and higher beam currents should provide access to the

spin-wave modes. If such experiments succeed, our understanding of the magnetic properties of ultrathin ferromagnetic films will be advanced substantially. It is our hope that the considerations here will stimulate such studies.

ACKNOWLEDGMENTS

This research was supported by the U.S. Department of Energy through Grant No. DE-FG03-84ER45083.

[1]For a study of the thermodynamics of ultrthin Fe films 1–4 ML of W(100), see M. Przybylski, I. Kaufman, and U. Gradmann, Phys. Rev. B **39**, 10 430 (1989).

[2]M. Bander and D. L. Mills, Phys. Rev. B **38**, 12 015 (1988); R. P. Erickson and D. L. Mills, *ibid.* **43**, 10 715 (1991); P. Krams, F. Lauks, R. L. Stamps, B. Hillebrands, and G. Guntherodt, *ibid.* **69**, 3674 (1992).

[3]R. P. Erickson and D. L. Mills, Phys. Rev. Rev. B **39**, 10 430 (1989); Phys. Rev. B **44**, 11 825 (1991); P. Politi, M. G. Pini, and A. Rettori, *ibid.* **46**, 8312 (1992).

[4]C. Herring and C. Kittel, Phys. Rev. **81**, 861 (1951).

[5]T. Izuyama, D. J. Kim, and R. Kubo, J. Phys. Soc. Jpn. **18**, 1025 (1963); C. Herring, in *Magnetism*, Vol. IV, edited by H. Suhl and G. Rado (Academic, New York, 1967).

[6]J. Kirschner, Phys. Rev. Lett. **55**, 973 (1985); A. Venus, and J. Kirschner, Phys. Rev. B **37**, 2199 (1988); Y. U. Idzerda, D. M. Lind, D. A. Papaconstantantopoulos, G. A. Prinz, B. T. Lonker, and J. J. Krebs, Phys. Rev. Lett. **61**, 1222 (1988); J. Appl. Phys. **64**, 5921 (1988); D. L. Abraham and H. Hopster, Phys. Rev. Lett. **62**, 1157 (1989).

[7]For examples of light scattering studies, see P. Grunberg, R. Schrieber, Y. Pang, M. B. Brodsky, and H. Sowers, Phys. Rev. Lett. **57**, 2442 (1986); and J. R. Dutcher, J. F. Cochran, I. Jacob, and W. G. Egelhoff, Jr., Phys. Rev. B **39**, 10 430 (1989).

[8]Examples of ferromagnetic resonance studies are as follows: B. Heinrich, S. T. Purcell, J. R. Dutcher, K. B. Urquhart, J. F. Cochran, and A. S. Arrott, Phys. Rev. B **38**, 12 879 (1988); and B. Heinrich, Z. Celinski, J. F. Cochran, W. B. Muir, J. Rudd, Q. M. Zhang, A. S. Arrott, K. Myrtle, and J. Kusihner, Phys. Rev. Lett. **64**, 673 (1990).

[9]A. Griffin and G. Gumbs, Phys. Rev. Lett. **37**, 371 (1976); G. Gumbs and A. Griffin, Surf. Sci. **91**, 669 (1980).

[10]J. Mathon, Phys. Rev. B **24**, 6588 (1981).

[11]P. Lederer and D. L. Mills, Phys. Rev. **160**, 590 (1967).

[12]Y. Nagaoka, Phys. Rev. **147**, 392 (1966).

[13]W. von der Linden and D. M. Edwards, J. Phys. Condens. Matter **3**, 4917 (1991).

[14]J. A. Henderson, J. Oitmaa, and M. C. B. Ashley, Phys. Rev. B **46**, 6328 (1992).

[15]S. R. Streight and D. L. Mills, Phys. Rev. B **37**, 965 (1988).

[16]See the discussion of Fe(100) in Sec. 1.4.1 of A. J. Freeman, C. L. Fu, S. Ohnishi, and M. Weinert, in *Polarized Electrons in Surface Physics,* edited by R. Feder (World Scientific, Singapore, 1985), p. 3; the (110) surface of Fe is discussed by C. L. Fui and A. J. Freeman, J. Magn. Magn. Mater. **69**, L1 (1987).

[17]J. Thomassen, F. May, B. Feldmann, M. Wuttig, and H. Ibach, Phys. Rev. Lett. **69**, 3831 (1993).

[18]J. Unguris, R. J. Celotta, and D. T. Pierce, Phys. Rev. Lett. **69**, 1125 (1992).

[19]T. G. Walker, A. W. Pang, H. Hopster, and S. F. Alvarado, Phys. Rev. Lett. **69**, 1121 (1992).

[20]M. P. Gokhale, A. Ormeci, and D. L. Mills, Phys. Rev. B **46**, 8978 (1992).

[21]See the paper by Abraham and Hopster cited in Ref. 6, along with H. Hopster and D. Abraham, Phys. Rev. B **40**, 7054 (1989).

[22]D. L. Hills, Phys. Rev. B **34**, 6099 (1986).

[23]Calculations of the bulk exchange splitting in Ni have been reported by J. W. D. Connolly, Phys. Rev. **159**, 415 (1967) and C. S. Wang and J. Callaway, Phys. Rev. B **15**, 298 (1977).

[24]For a recent example, see M. Balden, S. Lehwald, H. Ibach, A. Ormeci, and D. L. Mills, Phys. Rev. B **46**, 8978 (1992).

[25]M. L. Xu, B. M. Hall, S. Y. Tong, M. Rocca, H. Ibach, S. Lehwald, and J. E. Black, Phys. Rev. Lett. **54**, 1171 (1985); Burl M. Hall and D. L. Mills, Phys. Rev. B **34**, 8318 (1986).